Advanced echocardiographic imaging in valvular and systemic diseases

Wijngaarden, S.E. van

PART I

Utility and implications of advanced echocardiography in mitral regurgitation

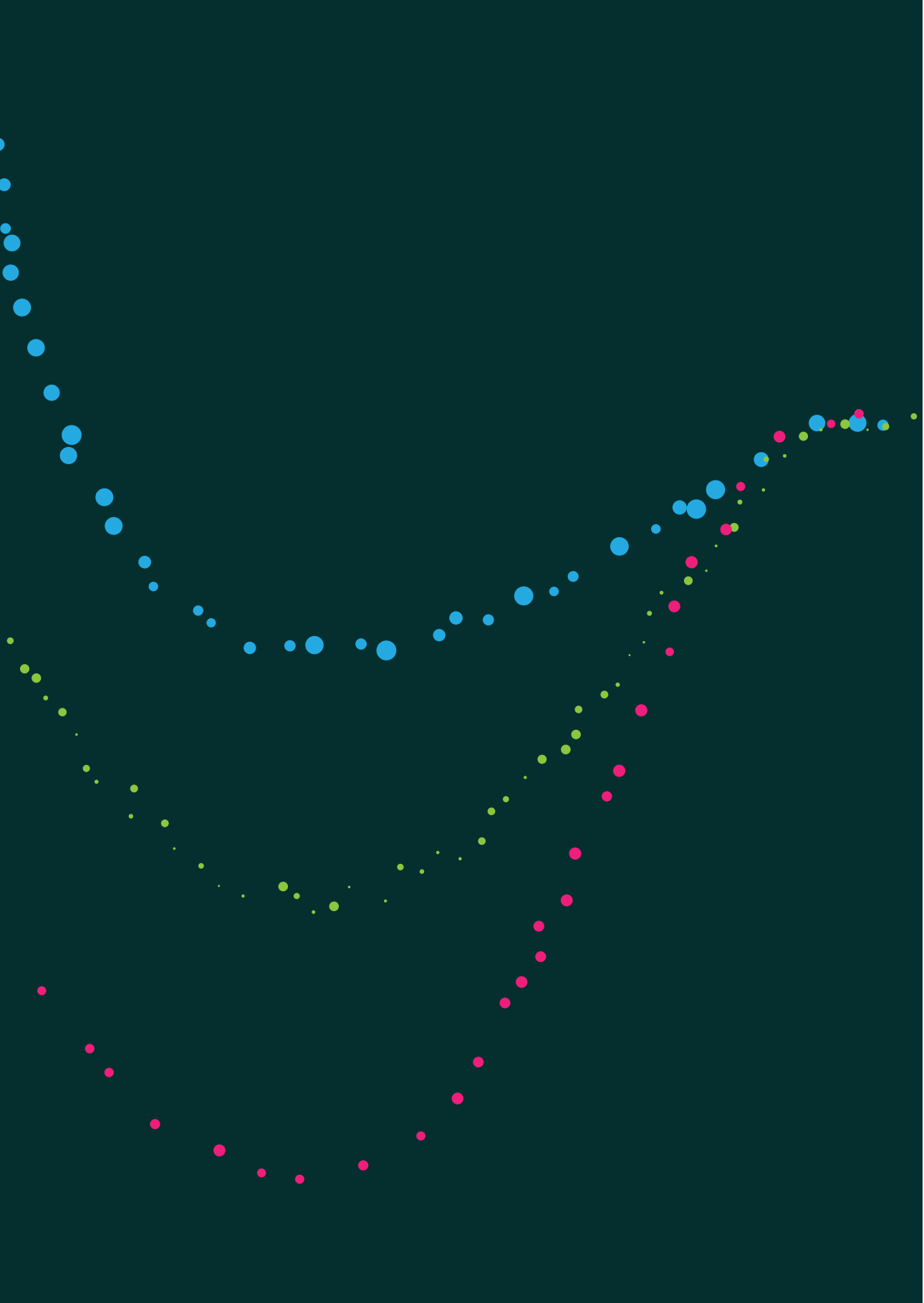

CHAPTER 2

Regional Left Ventricular Myocardial Mechanics in Degenerative Myxomatous Mitral Valve Disease: a Comparison Between Fibroelastic Deficiency and Barlow's Disease

Suzanne E. van Wijngaarden, MD; Rachid Abou, MD; Yasmine L. Hiemstra, MD; Nina Ajmone Marsan, MD, PhD; Jeroen J. Bax, MD, PhD; Victoria Delgado, MD, PhD

JACC Cardiovasc Imaging. 2018;11:1362-1364, published as a short article

ABSTRACT

Objectives: The aim of this study was to evaluate differences in regional Left ventricular (LV) longitudinal strain between fibro-elastic deficiency (FED) and Barlow's disease (BD) using 2-dimensional (2D) speckle tracking echocardiography.

Background: LV mechanics may differ between various etiologies of degenerative mitral regurgitation (MR) and contribute to the mechanism of valve regurgitation. Speckle tracking echocardiography permits assessment of regional myocardial strain.

Methods: In total 104 patients with moderate and severe, primary MR (62±11 years, 66 male, 62 FED and 42 BD) and 40 control subjects (62±14 years, 20 male) were evaluated. Basal, mid and apical LV longitudinal strains were assessed with 2D speckle tracking echocardiography. FED, BD and control subjects were compared using linear mixed models corrected for age, sex, LV end-systolic and end-diastolic volumes.

Results: Basal to apical LV longitudinal strains showed a distinct pattern across the groups: in FED, LV basal longitudinal strain was impaired (-14.7%±3.5 versus -17.8%±1.4, $p<0.001$) whereas apical longitudinal strain was enhanced (-27.5%±4.6 versus -26.4%±2.5, $p=0.021$) compared to controls. In contrast, BD patients had enhanced LV longitudinal strain values of the basal level compared to controls (-19.9%±2.6 versus -17.8%±1.4, $p=0.034$) and to FED patients (-19.9%±2.6 versus -14.7%±3.5, $p<0.001$).

Conclusions: Regional LV mechanics as assessed with 2D speckle tracking echocardiography shows distinct patterns in FED and BD: FED is characterized by impaired longitudinal strain of the basal LV segments and enhanced longitudinal strain of the apical segments whereas BD patients show enhanced LV strain of the basal segments. This suggests that in FED patients the valvular incompetence may be caused exclusively by a valvular problem whereas in BD patients, the hyper-enhanced function of the LV basal segments may contribute to secondary, functional prolapse of both leaflets.

INTRODUCTION

Degenerative myxomatous mitral valve disease is the most prevalent cause of mitral regurgitation (MR) in Europe (1) and is primarily characterised by degenerative changes of the mitral valve apparatus that lead to excessive motion of the leaflets(2). These degenerative changes of the mitral valve leaflets encompass fibroelastic deficiency (FED), characterized by thin leaflets and a ruptured chord due to collagen deficiency, to Barlow's disease (BD) which is characterized by large and thickened leaflets, with excessive tissue and elongated and frequently ruptured chords (3). Additionally, the mitral dynamics of the mitral annulus in degenerative mitral valve disease are characterised by increased motility during systole (4-6). Moreover, patients with BD have a notable enhanced motility and excessive flattening of the saddle-shaped mitral annulus at late systole in comparison to patients with FED (4). This characteristic mitral annulus motion in patients with BD may be related to enhanced function of the basal segments of the left ventricle (LV) and it has been hypothesized that fixation of the hyper-enhanced dynamics of the mitral annulus with a ring annuloplasty may be sufficient to restore the competence of the mitral valve.

Two-dimensional (2D) speckle tracking echocardiography permits assessment of global and regional multidirectional myocardial strain. In patients with mitral regurgitation, LV global longitudinal strain (GLS) has been shown to detect subtle changes in LV systolic dysfunction (7-9). By characterising regional LV longitudinal strain, differences in LV mechanics between patients with severe MR due to FED versus patients with BD could be evaluated. We hypothesized that patients with BD have hyper-enhanced LV longitudinal strain of the basal segments as compared with patients with FED, causing further dilation of the annulus, leaflet malcoaptation and increased regurgitant volume during late systole. This would support the hypothesis that by fixing the mitral annulus with an annuloplasty ring the competence of the mitral valve can be restored.

METHODS

Patients

A total of 104 patients with moderate-to-severe and severe, degenerative myxomatous MR were evaluated. Patients were divided into two groups according to the underlying pathophysiology: FED (N=62) and BD (N=42). FED was defined as MR caused by one single prolapsing segment of the mitral leaflet. BD was defined as a multi-segment

leaflet prolapse characterised by diffuse thickening and excessive tissue (10, 11). In addition, a control group of 40 patients with structurally and functionally normal heart and mitral valve were included. Exclusion criteria were patients with ischemic heart disease, rheumatic heart disease, pervious bacterial endocarditis, associated connective tissue disorder, hypertrophic cardiomyopathy and mitral annulus calcification. Clinical characteristics were retrospectively collected from the departmental cardiology information system (EPD-Vision; Leiden University Medical Center, Leiden, The Netherlands). The institutional ethical committee approved this retrospective analysis of clinically collected data and waived the need for patient written informed consent.

Two-dimensional echocardiography

Transthoracic echocardiography was performed using a commercially available system (E9; General Electric-Vingmed, Horten, Norway). Using a 5MS transducer, images of the standard parasternal and apical views were obtained with the patient in the left lateral decubitus position. M-mode and 2D, colour, pulsed and continuous wave Doppler data were stored in cine-loop format. Retrospective offline analysis was performed using commercially available post-processing data software (EchoPAC BT13; GE Medical Systems, Horten, Norway).

Left ventricular dimensions were measured in M-mode recordings in diastole and included interventricular septal thickness, LV end-diastolic diameter and posterior wall thickness. Left atrial (LA) anteroposterior diameter was measured on M-mode recordings during LV systole. Left ventricular ejection fraction (LVEF), LV end-diastolic (LVEDV) and end-systolic (LVESV) volumes were measured in the apical 2- and 4- chamber views according to the current guidelines using the biplane Simpson's method (12).

To assess LV diastolic function peak early (E) and late (A) diastolic velocities measured on pulsed wave Doppler recordings of the transmitral flow were measured and the E/A ratio was calculated(13). Additionally, E-prime was measured with tissue Doppler imaging at the lateral and septal sides of the mitral annulus in the apical four-chamber view and E/E' ratio was calculated.

The systolic pulmonary arterial pressure (sPAP) was estimated by measuring the tricuspid regurgitation peak velocity on continuous wave Doppler recordings. The right atrial pressure estimated by the inferior vena cava diameter and degree of respiratory collapse

were also taken into consideration to estimate the sPAP (14).

Mitral regurgitation grade was assessed according to current recommendations using colour, continuous and pulsed wave Doppler recordings of the mitral valve. Qualitative, semiquantitative and quantitative parameters were evaluated. The effective regurgitant orifice area (EROA) and regurgitant volume were quantified using the proximal isovelocity surface area method (15).

Two-dimensional speckle tracking strain echocardiography

Two-dimensional speckle tracking strain echocardiography permits quantification of myocardial deformation (strain) by tracking acoustic speckles in every frame during the cardiac cycle (16). Longitudinal LV strain was measured in the standard apical two-, three- and four-chamber views and LV GLS was obtained as the average of the longitudinal strain values of 17 segments and displayed in a bulls-eye plot (Figure 1). Peak systolic LV strain values for each LV level (basal, mid and apical) were separately calculated. LV strain values are expressed as negative values and a more negative value represents better myocardial systolic function.

Statistical analysis

Statistical analyses were performed using the SPSS® software version 23.0 (IBM, Armonk, NY, USA). Continuous variables are presented as mean ± standard deviation or as median with interquartile ranges (IQR) according to the distribution. Categorical data are reported as frequencies and percentages. Continuous variables were compared using the one-way analysis of variance, applying the Bonferroni's post-hoc analysis, the Kruskall-Wallis one-way analysis of variance or the Mann-Whitney U-test, as appropriate. Categorical data were compared using the Chi-square test. Left ventricular strain for the basal, mid and apical levels were compared between controls, FED and BD with linear mixed models corrected for age, sex, LVEDV and LVESV. A p-value<0.05 was considered statistically significant.

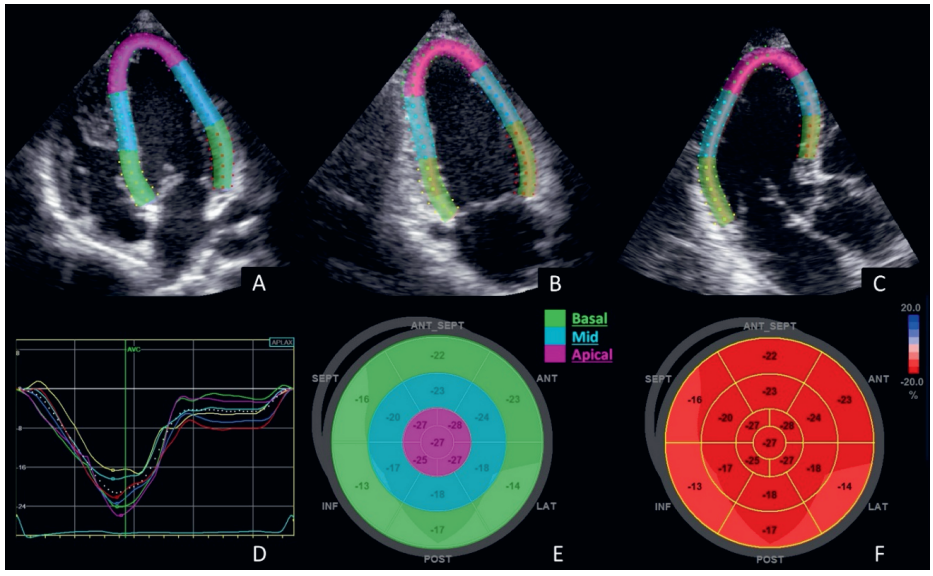

Figure 1. Left ventricular global and per-level longitudinal strain analysis.
Measurement of longitudinal strain with 2-dimensional speckle tracking strain analysis applied to a four-chamber apical view (A), two-chamber apical view (B) and a three-chamber apical view (C). D: curves of longitudinal strain per segment and the average (dotted line). E: Bull's eye display of all LV levels, green corresponding to basal, blue to mid and purple to apical levels; F: Bull's eye display in which strain value is colour coded; dark red represents more enhanced strain and lighter red represents more reduced strain.

RESULTS

Patients

Patient characteristics are summarized in Table 1. There were no significant differences across the groups for age and sex. Compared with controls and BD patients, FED patients had more frequently atrial fibrillation, worse New York Heart Association functional class and received more frequently diuretics. Both FED and BD patients received more often angiotensin-converting-enzyme inhibitors or angiotensin-II receptor blockers compared to controls.

Table 1. Clinical characteristics.

Characteristics	Controls (n=40)	FED (n=62)	BD (n=42)	ANOVA p value
Age , years	62 ± 14	64 ± 10	59 ± 12	0.059
Male, n (%)	19 (48)	39 (63)	27 (64)	0.216
BSA, m^2	1.88 ± 0.19	1.94 ± 0.20	1.97 ± 0.24	0.134
Prior MI, n (%)	0 (0)	2 (3)	2 (5)	0.406
Atrial fibrillation, n (%)	0 (0)	15 (24)*	3 (7)†	0.001
Hypertension, n (%)	18 (45)	28 (45)	18 (43)	0.970
Hypercholesterolemia, n (%)	5 (13)	12 (19)	6 (14)	0.614
Diabetes Mellitus, n (%)	2 (5)	4 (7)	3 (7)	0.919
(Ex-)Smoker, n (%)	12 (30)	24 (39)	13 (32)	0.611
COPD, n (%)	0 (0)	0 (0)	3 (7)	0.747
NYHA class, n (%)				<0.001
I	40 (100)	18 (29)	12 (29)	
II	0 (0)	23 (37)	22 (52)	
III/IV	0 (0)	21 (34)	8 (19)	
eGFR (ml/min/1.73m^2)	85 ± 17	83 ± 21	89 ± 20	0.278
Medications				
ACEi/ARB, n (%)	10 (25)	32 (52)*	24 (57)*	0.007
Beta-blocker, n (%)	10 (25)	29 (47)	18 (43)	0.079
Ca^{2+} channel blocker, n (%)	7 (18)	10 (16)	3 (7)	0.805
Statin, n (%)	6 (15)	21 (34)	9 (21)	0.081
Diuretics, n (%)	6 (15)	24 (39)*	7 (17)†	0.008

* Indicates a significant p value versus controls; † indicates a significant p value versus FED; ACEi, angiotensin-converting-enzym inhibitor; ARB, angiotensin-II receptor blocker; BD, Barlow's disease; BSA, body surface area; COPD, chronic obstructive pulmonary disease; eGFR, estimated glomerular filtration rate; FED, fibroelastic deficiency; MI, myocardial infarction; NYHA, New York Heart Association.

Conventional 2D echocardiography

The echocardiographic results are summarized in Table 2. FED patients had a significantly lower LVEF compared to both BD and controls. Compared with controls, FED and BD patients showed larger LV and LA dimensions and worse LV diastolic dysfunction.

Table 2. Echocardiographic characteristics.

2D Echocardiographic parameters	Controls (n=40)	FED (n=62)	BD (n=42)	ANOVA p value
Conventional parameters				
IVST (mm)	10 ± 2	10 ± 2	10 ± 2	0.433
LVEDd (mm)	48 ± 5	57 ± 7*	57 ± 8*	<0.001
PWT (mm)	10 ± 1	10 ± 2	10 ± 2	0.134
LA diameter (mm)	34 ± 5	47 ± 8*	46 ± 7*	<0.001
LVEF (%)	63 ± 5	58 ± 8*	62 ± 7†	0.001
LVEDV (ml)	98 (87 – 110)	142 (102 – 164)*	150 (120 – 171)*	<0.001
LVESV (ml)	36 (26 – 43)	58 (44 – 75)*	58 (46 – 72)*	<0.001
E/A ratio	0.95 (0.76 – 1.09)	1.46 (1.01 – 2.09)*	1.41 (1.19 – 1.91)*	<0.001
E-prime cm/sec	12.2 ± 2.0	9.6 ± 2.9	9.4 ± 2.9	0.402
E/E' ratio	6.7 (5.7 – 9.0)	11.5 (8.3 – 15.7)*	10.5 (9.0 – 13.6)*	<0.001
sPAP (mmHg)	24 ± 8	38 ± 15*	29 ± 7*†	<0.001
EROA (mm^2)	-	34 (26 – 52)	39 (25 – 59)	0.093
Regurgitant volume (ml)	-	52 ± 17	46 ± 18	0.160
Speckle tracking strain analysis				
LV GLS (%)	-21.5 ± 1	-19.8 ± 3	-21.4 ± 3	0.091

*Indicates a significant p value versus controls; † indicates a significant p value versus FED; LV GLS was corrected for age, sex, LVEDV and LVESV in a univariate model; BD, Barlow's disease; EROA, effective regurgitant orifice area; FED, fibroelastic deficiency; GLS, global longitudinal strain; IVRT, isovolumic relaxation time; IVST, interventricular septum thickness; LA, left atrial; LV, left ventricular; LVEDV, left ventricular end-diastolic volume; LVEF, left ventricular ejection fraction; LVESV, left ventricular end-systolic volume; PWT, posterior wall thickness; sPAP, systolic pulmonary artery pressure; TAPSE, tricuspid annular plane systolic excursion

2D speckle tracking strain analysis

There were no differences in LV GLS across the groups after correcting for age, sex, LVEDV and LVESV. In per-LV level analysis, LV longitudinal strain increased (better function) from base to apex (Figure 2) in all three groups showing that the myocardial segments of the basal level have less pronounced deformation than the apical segments. This gradient in LV longitudinal strain was significantly different across the groups: FED patients showed significantly more impaired LV longitudinal strain values at the basal level but significantly enhanced LV longitudinal strain values at the apical level as compared with controls (LV longitudinal strain basal level: -14.7% ± 3.5 versus -17.8% ± 1.4, p<0.001 and LV longitudinal strain apical level: -27.5% ± 4.6 versus -26.4% ± 2.5, p=0.021; respectively). In contrast, BD patients had hyper-enhanced LV strain values of the basal level compared to controls (-19.9% ± 2.6 versus -17.8% ± 1.4, p=0.034) and to FED patients (-19.9% ± 2.6 versus -14.7% ±

3.5, p<0.001), with similar values in the mid and apical levels compared to controls and FED patients. Figure 3 illustrates the differences in regional LV longitudinal strain between FED and BD. These findings confirm our hypothesis and suggest that in FED patients the valvular incompetence may be caused exclusively by a valvular problem whereas in BD patients, the hyper-enhanced function of the LV basal segments may contribute to functional prolapse of both leaflets.

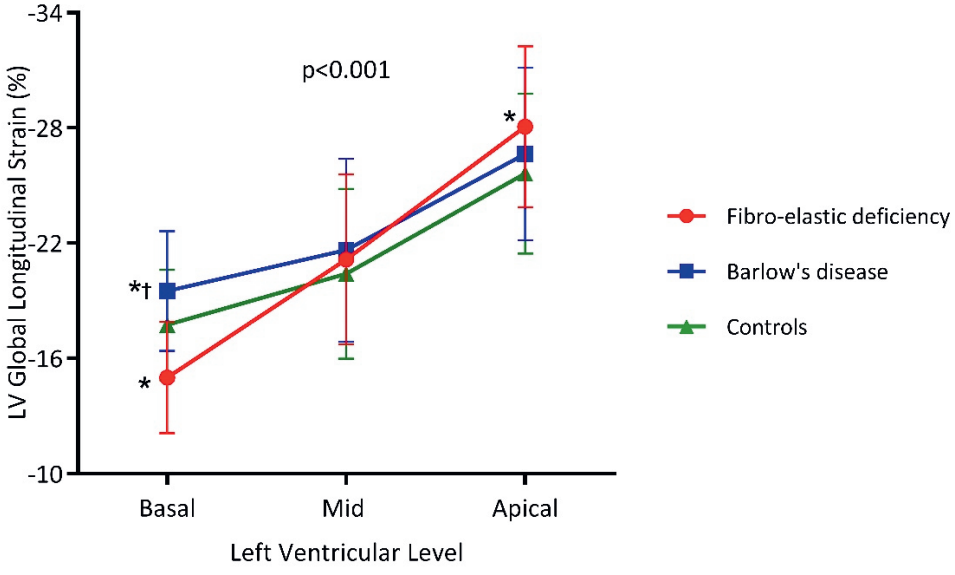

Figure 2. Comparison of longitudinal strain values per left ventricular level

** Indicates a significant p value versus the same level in controls; † Indicates a significant p value in Barlow's disease versus Fibro-elastic deficiency; A linear mixed model corrected for age, gender, and LV end-diastolic and end-systolic volumes was applied. The results are displayed as mean and standard errors. LV; left ventricular*

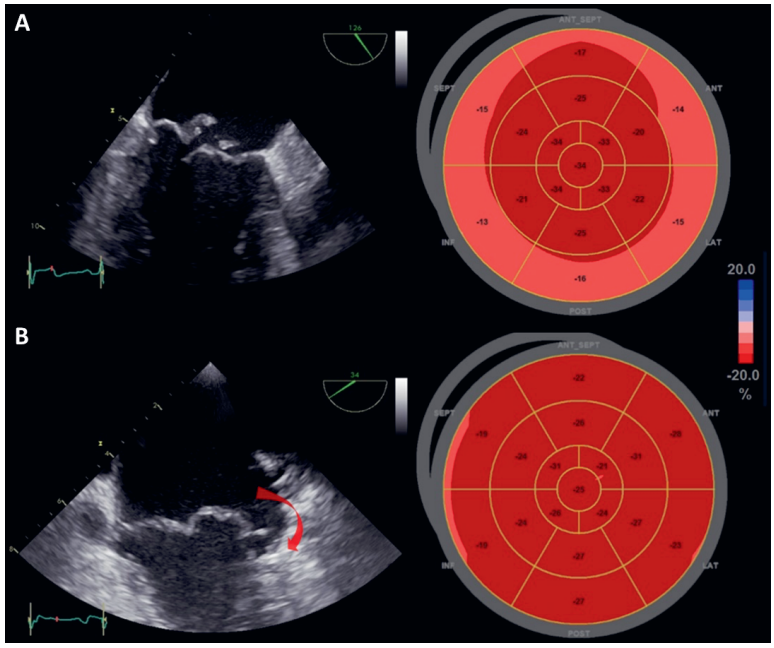

Figure 3. Per-level left ventricular longitudinal strain in fibroelastic deficiency and Barlow's disease. *Transesophageal echocardiographic view of fibroelastic deficiency (FED) patient (A) and Barlow's disease patient (B) and corresponding bulls' eye plots with longitudinal strain values per level. Note that in the FED patient, the basal level shows more impaired myocardial longitudinal strain values as compared with the Barlow's disease patient. The enhanced myocardial longitudinal shortening of the basal level in Barlow's disease patient may contribute further to the incompetence of the mitral valve by pulling down the insertion of the mitral leaflet (arrow).*

DISCUSSION

The present study demonstrates the different patterns in the basal to apical gradient in LV longitudinal strain in FED versus BD patients. While BD patients showed hyper-enhanced LV longitudinal strain in the basal segments, FED patients showed impaired basal LV longitudinal strain. This suggests that MR in BD patients can be influenced by abnormally hyper-contractile basal LV segments that further dilate the mitral annulus leading to mitral valve incompetence whereas in FED patients, the MR mechanism is primarily valvular.

Mitral valve dynamics in fibroelastic deficiency versus Barlow's disease: interplay with regional left ventricular strain

Differences in leaflet structure and mitral annulus dynamics between FED and BD causing MR have been described previously (4-6, 17). Using 3-dimensional modelling software, it has been demonstrated that the mitral annulus dynamics in patients with primary MR caused by FED or BD differ from those of healthy individuals with normal mitral valves. In healthy subjects, the LV forces fold the saddle-shaped mitral annulus during systole in order to relieve stress on the leaflets (18, 19). In contrast, FED and BD patients with significant MR characteristically show a more dynamic mitral annulus during systole with excessive annular dilatation and folding and flattening of the saddle-shaped annulus (4). Especially in BD patients, these increased dynamics are mainly observed in the commissural width and are characterised by folding of the saddle-shaped annulus at late systole. Normally, the diameter between the commissures remains unchanged, however, in BD, this diameter shows increased dilatation towards late systole which is accompanied by increased flattening of the annulus. Since mitral annulus dynamics are naturally subject to LV forces, abnormal regional LV myocardial function may have an important role in changes of mitral annulus dynamics. The present study demonstrates that in BD patients, the basal LV segments show hyper-enhanced LV longitudinal strain which may explain why the mitral annulus is hyper-dynamic at late systole. The mitral annulus is subject to increased LV dynamics and is pulled outward at late systole which leads to annular dilatation and leaflet malcoaptation.

Few studies have assessed the relationship between regional LV mechanics and degenerative MR (20, 21). Using 2D speckle tracking echocardiography, Fukuda et al evaluated regional (basal, mid and apical) LV strains in 130 patients with primary MR and in 30 controls (20). Patients with primary MR showed larger LV basal diameter and impaired LV longitudinal strain of the basal LV segments as compared with controls. These alterations were restored after mitral valve repair using mitral ring annuloplasty (20). In addition, Huttin et al showed in 100 patients with mitral valve prolapse, the presence of abnormal LV strain in the LV segments characterised by increased post-systolic shortening (further longitudinal shortening beyond the aortic valve closure) (21). However, no distinction was made between FED and BD in these studies. In contrast, the present study is the first to

characterise regional LV strain in these two etiologies of degenerative myxomatous mitral valve disease.

Clinical implications

In MR patients, the decision making for timing of surgery and type of surgical technique are challenging. Currently, MR severity, clinical symptoms, LV dimensions and function and LA dimensions are the main determinants of surgical treatment indication (2, 11). When surgical mitral valve repair with an annuloplasty ring is performed, MR is eliminated by correcting the leaflet prolapse and stabilizing the mitral annulus. Implantation of a ring has shown to significantly alter the geometry of the basal LV myocardium and reduce myocardial stress (22). However, better understanding of LV mechanics and its relation to mitral annulus dynamics in FED and BD may have an important impact for the development of specific surgical techniques. For example, in BD implantation of an annuloplasty ring may restore mitral annulus dynamics and normalize leaflet stress. In contrast, in FED patients the addition of an annuloplasty ring may be debatable if the mitral annulus is not dilated and the dynamics are preserved (23-25). For this purpose, virtual simulation studies have shown promising results in reproducing and predicting mitral annulus dynamics with different ring types(26, 27). These simulations may also help in the development of specific surgical rings personalized for each individual patient.

Limitations

The measurements of LV strain were performed using a dedicated post-processing software (2D speckle tracking strain echocardiography). Whether the measurements are consistent with other vendors was not assessed. Due to the small sample size, the present study should be considered as a hypothesis generating study and further validation with larger study populations is necessary.

Conclusion

In patients with degenerative MR, a different pattern in regional LV longitudinal strain is observed according to the underlying pathophysiology: while in BD, there is an hyper-enhanced LV longitudinal strain of the basal segments, in FED, the basal LV segments show impaired longitudinal strain. This suggests a functional component in the mechanism

of MR in BD patients whereas in FED the pathology is primarily valvular.

Reference List

1. Iung B, Baron GF, Butchart EG, et al. A prospective survey of patients with valvular heart disease in Europe: The Euro Heart Survey on Valvular Heart Disease. Eur Heart J 2003;24:1231-43

2. Lancellotti P, Tribouilloy C, Hagendorff A, et al. Recommendations for the echocardiographic assessment of native valvular regurgitation: an executive summary from the European Association of Cardiovascular Imaging. Eur Heart J Cardiovasc Imaging 2013; 14:611-44.

3. Adams DH, Rosenhek R, Falk V. Degenerative mitral valve regurgitation: best practice revolution. Eur Heart J 2010; 31:1958-66.

4. van Wijngaarden SE, Kamperidis V, Regeer MV, et al. Three-dimensional assessment of mitral valve annulus dynamics and impact on quantification of mitral regurgitation. Eur Heart J Cardiovasc Imaging 2017 Feb 7 [E-pub ahead of print], https://doi.org/10.1093/ehjci/jex001.

5. Grewal J, Suri R, Mankad S, et al. Mitral annular dynamics in myxomatous valve disease: new insights with real-time 3-dimensional echocardiography. Circulation 2010; 121:1423-31.

6. Clavel MA, Mantovani F, Malouf J, et al. Dynamic phenotypes of degenerative myxomatous mitral valve disease: quantitative 3-dimensional echocardiographic study. Circ Cardiovasc Imaging 2015; 8.

7. Witkowski TG, ten Brinke EA, Delgado V, et al. Surgical ventricular restoration for patients with ischemic heart failure: determinants of two-year survival. Ann Thorac Surg 2011; 91:491-8.

8. Kamperidis V, Marsan NA, Delgado V, Bax JJ. Left ventricular systolic function assessment in secondary mitral regurgitation: left ventricular ejection fraction vs. speckle tracking global longitudinal strain. Eur Heart J 2016; 37:811-6.

9. Lee R, Marwick TH. Assessment of subclinical left ventricular dysfunction in asymptomatic mitral regurgitation. Eur J Echocardiogr 2007; 8:175-84.

10. Anyanwu AC, Adams DH. Etiologic classification of degenerative mitral valve disease: Barlow's disease and fibroelastic deficiency. Semin Thorac Cardiovasc Surg 2007; 19:90-6.

11. Vahanian A, Alfieri O, Andreotti F, et al. Guidelines on the management of valvular heart disease (version 2012): the Joint Task Force on the Management of Valvular Heart Disease of the European Society of Cardiology (ESC) and the European Association for Cardio-Thoracic Surgery (EACTS). Eur J Cardiothorac Surg 2012; 42:S1-44.

12. Lang RM, Badano LP, Mor-Avi V, et al. Recommendations for cardiac chamber quantification by echocardiography in adults: an update from the American Society of Echocardiography and the European Association of Cardiovascular Imaging. Eur Heart J Cardiovasc Imaging 2015; 16:233-70.

13. Nagueh SF, Smiseth OA, Appleton CP, et al. Recommendations for the Evaluation of Left Ventricular Diastolic Function by Echocardiography: An Update from the American Society of Echocardiography and the European Association of Cardiovascular Imaging. Eur Heart J Cardiovasc Imaging 2016; 17:1321-60.

14. Kircher BJ, Himelman RB, Schiller NB. Noninvasive estimation of right atrial pressure from the inspiratory collapse of the inferior vena cava. Am J Cardiol 1990; 66:493-6.

15. Grayburn PA, Carabello B, Hung J, et al. Defining "severe" secondary mitral regurgitation: emphasizing an integrated approach. J Am Coll Cardiol 2014; 64:2792-801.

16. Delgado V, Ypenburg C, van Bommel RJ, et al. Assessment of left ventricular dyssynchrony by speckle tracking strain imaging comparison between longitudinal, circumferential, and radial strain in cardiac resynchronization therapy. J Am Coll Cardiol 2008; 51:1944-52.

17. Dal-Bianco JP, Beaudoin J, Handschumacher MD, Levine RA. Basic mechanisms of mitral regurgitation. Can J Cardiol 2014; 30:971-81.

18. Lee AP, Hsiung MC, Salgo IS, et al. Quantitative analysis of mitral valve morphology in mitral valve prolapse with real-time 3-dimensional echocardiography: importance of annular saddle shape in the pathogenesis of mitral regurgitation. Circulation 2013; 127:832-41.

19. Salgo IS, Gorman JH, III, Gorman RC, et al. Effect of annular shape on leaflet curvature in reducing mitral leaflet stress. Circulation 2002; 106:711-7.

20. Fukuda S, Song JK, Mahara K, et al. Basal Left Ventricular Dilatation and Reduced Contraction in Patients With Mitral Valve Prolapse Can Be Secondary to Annular Dilatation: Preoperative and Postoperative Speckle-Tracking Echocardiographic Study on Left Ventricle and Mitral Valve Annulus Interaction. Circ Cardiovasc Imaging 2016; 9.

21. Huttin O, Pierre S, Venner C, et al. Interactions between mitral valve and left ventricle analysed by 2D speckle tracking in patients with mitral valve prolapse: one more piece to the puzzle. Eur Heart J Cardiovasc Imaging 2017; 18:323-31.

22. Morrel WG, Ge L, Zhang Z, Grossi EA, Guccione JM, Ratcliffe MB. Effect of mitral annuloplasty device shape and size on leaflet and myofiber stress following repair of posterior leaflet prolapse: a patient-specific finite element simulation. J Heart Valve Dis 2014; 23:727-34.

23. Seeburger J, Kuntze T, Mohr FW. Gore-tex chordoplasty in degenerative mitral valve repair. Semin Thorac Cardiovasc Surg 2007; 19:111-5.

24. De Bonis M, Lapenna E, Maisano F, et al. Long-term results (</=18 years) of the edge-to-edge mitral valve repair without annuloplasty in degenerative mitral regurgitation: implications for the percutaneous approach. Circulation 2014; 130:S19-S24.

25. Falk V, Seeburger J, Czesla M, et al. How does the use of polytetrafluoroethylene neochordae for posterior mitral valve prolapse (loop technique) compare with leaflet resection? A prospective randomized trial. J Thorac Cardiovasc Surg 2008; 136:1205-6.

26. Choi A, McPherson DD, Kim H. Computational virtual evaluation of the effect of annuloplasty ring shape. Int J Numer Method Biomed Eng 2016. [E-pub ahead of print], https://doi.org/10.1002/cnm.2831

27. Rim Y, Choi A, McPherson DD, Kim H. Personalized Computational Modeling of Mitral Valve Prolapse: Virtual Leaflet Resection. PLoS One 2015; available at: https://doi.org/10.1371/journal.pone.0130906